

Vicarious satellite calibration in the solar spectral range by means of calculated radiances and its application to Meteosat

Peter Koepke

The method of vicarious calibration by means of calculated radiances allows absolute calibration of satellite radiometers in orbit. It works by comparing counts from the radiometer to be calibrated with corresponding absolute radiances, calculated from actual values of the relevant optically acting parameters of the atmosphere and the earth's surface. The method is applied to the VIS-channel (it measures in the visible and near IR) of the European geostationary satellite Meteosat-1. To minimize uncertainties, the procedure is carried out over different surfaces, at different atmospheric conditions, and at different sun and satellite angles. The ratio between the effective radiances (the radiances at the satellite weighted with its spectral response) and the measured 6-bit counts of the Meteosat-1-VIS-channel is the calibration constant $c_{\text{sat}} = 2.66 \text{ W} \cdot \text{m}^{-2} \cdot \text{sr}^{-1}/\text{count}$. The accuracy of the calibration is $\pm 6\%$. The inaccuracy is mainly due to the broad digitization steps of the channel. Conversion factors are presented which allow one to calculate from the effective radiance the radiance at the satellite (the radiance leaving the atmosphere).

I. Introduction

The quantitative analysis of images produced by satellite-borne radiometers requires knowledge of their calibration. Since the application of modern satellite data requires higher quantitative validity, there is a real need to solve the calibration problem.¹ Absolute in-flight calibration can be done in two ways: (1) with an onboard calibration system, i.e., blackbody, cavity, known light source, solar radiation, or (2) by "vicarious calibration"¹ where a portion of the earth viewed by the instrument becomes a calibration source.

The calibration should include all optical elements of the radiometer, including the primary optic, which often has a large diameter, especially for geostationary satellites. From this point of view, calibration with onboard systems may cause technical difficulties. Vicarious calibration, however, allows calibration of the complete instrument. Beside this possibility of checking onboard calibration systems, vicarious calibration is useful for calibrating meteorological satellites, which are designed for image interpretation only and have no onboard calibration system.

Vicarious calibration can be performed in two ways: (1) by comparing the counts from the radiometer to be calibrated with data from a similar calibrated radiometer carried by an aircraft or satellite,²⁻⁵ or (2) by comparing the counts from the radiometer to be calibrated with the corresponding radiances, calculated from the values of the actual optically acting parameters of the atmosphere and the earth's surface. This vicarious calibration by means of calculated radiances can be applied in every spectral region where the radiative transfer equation can be solved and the actual parameters are known.^{6,7} In this paper use of the method in the solar spectral region is presented, applied to the calibration of the VIS-channel of the European geostationary satellite Meteosat-1.⁸ Information on the properties of the satellite is in Sec. IV.

II. Method

For a specific count, as measured by the radiometer to be calibrated, all corresponding optically acting parameters of the atmosphere and the underlying surface are determined. Based on these data, the absolute radiance L_T (see Table I for a complete list of symbols in this paper) leaving the top of the atmosphere and measured by the satellite is calculated. Comparison of one count with its corresponding radiance gives a calibration value. Repeated comparison of different counts with their corresponding radiances give different calibration values, which are the desired absolute in-flight calibration.

The author is with Universitat München, Meteorologisches Institut, D-8 München 2, Federal Republic of Germany.

Received 13 October 1981.

0003-6935/82/152845-10\$01.00/0.

© 1982 Optical Society of America.

Table I. List of Symbols

E_{\odot}	Solar irradiance at the top of the atmosphere
L_{rec}	Upward emerging radiance from the top of the atmosphere, the radiance at the satellite, integrated over the wavelength between 0.4 and 1.1 μm [with rectangular spectral response equal to 1, Eq. (7)]
L_{sat}	Upward emerging radiance from the top of the atmosphere measured by Meteosat-VIS-channel, weighted with its spectral response [Eq. (2)], the effective radiance
L_{sol}	Upward emerging radiance from the top of the atmosphere, the radiance at the satellite, integrated over the total solar wavelength region [Eq. (5)]
L_T	Upward emerging radiance from the top of the atmosphere, the radiance at the satellite
T	Linke turbidity factor (total optical depth in multiples of Rayleigh optical depth)
c_{sat}	Calibration constant for the Meteosat-VIS-channels [Eqs. (3), (4), (10), and (11)]
f_{rec}	Conversion factor for calculating L_{rec} from L_{sat}
f_{sol}	Conversion factor for calculating L_{sol} from L_{sat}
h_{\odot}, h_{sat}	Elevation angle of sun, satellite
p	Scattering phase function
γ_r	Bidirectional reflection function
λ	Wavelength; converts a quantity into spectral quantity when used as a subscript
σ_a	Gas absorption coefficient
τ_{sat}	Relative spectral response of Meteosat-channels-VIS-1 and VIS-2
φ	Azimuth angle of satellite relative to sun's azimuth
$\tilde{\omega}$	Single-scattering albedo

Where the response is linear, the calibration values lie on a straight line, which slope is the calibration constant c :

$$L_T = c \cdot \text{count.} \quad (1)$$

Of course, the method is not restricted to a specific wavelength region.

In the solar spectral region, radiation leaving the atmosphere consists of photons originating from the sun and scattered in the atmosphere or reflected at the surface. So the spectral radiances from the top of the atmosphere $L_{T\lambda}$ depend on the angles among sun, target, and satellite, on the spectral irradiance of the extraterrestrial sun $E_{\odot\lambda}$ (corrected with a factor to take into account the varying distance between sun and earth during the year) and on the spectral optical properties of atmosphere and surface. In cloudless atmospheres, the relevant optical parameters are the turbidity (expressed as Linke turbidity factor T_{λ} or optical depth δ_{λ}), the scattering phase function P_{λ} and the single-scattering albedo $\tilde{\omega}_{\lambda}$ (both depending on aerosol size distribution and refractive index), the absorption coefficient $\sigma_{a\lambda}$ for absorption due to atmospheric gases, and the reflectance of the surface $\gamma_{r\lambda}$.

If all these parameters are known, the radiance to be measured by the satellite-borne radiometer can be calculated by solving the radiative transfer equation.⁹ Sites where the parameters are horizontal homogeneous are selected, because it makes calculation and data capture easier.

In practice, the method starts with a search for conditions where knowledge of the optical parameters is best or most simply achieved. From these data, radi-

ances can be calculated for any zenith and azimuth angle of sun and satellite derived from the position of satellite, target, and sun.

The first of these conditions is a cloudfree atmosphere, which is necessary to assume a homogeneous atmosphere and to eliminate microphysical parameters of clouds which are difficult to measure.

In many cloudfree cases, the surface reflectance dominates the upward radiances emerging from the top of the atmosphere. For the radiance calculation used in the vicarious calibration technique, it is, therefore, necessary to be precise with the reflectance, which means using the spectral bidirectional reflection functions.

Use of different surface types, each with different atmospheric turbidities and different solar zenith and azimuth angles, gives rise to independent calibration values. If the radiometer responds linearly, these values can be combined into a straight line, the slope of which is the resulting single calibration constant. If the radiometer can measure deep space, the resulting counts allow fixing of the intersection point of the straight line with the abscissa because the radiances from space can be assumed to be zero.

The method of vicarious calibration in the solar range, as mentioned above, can be used to calibrate any satellite-borne radiometer working in this spectral range.

III. Uncertainty in the Method

Uncertainty in the calibration results from uncertainty in the measured counts and in the calculated radiances. The more accurate these quantities are and the more calibration values are used to determine the calibration curve, the less is its uncertainty.

Of course, if counts from different parts of the image or different times are used to derive the calibration curve, the response of the radiometer is assumed to be stable over the image for the duration of the calibration. On the other hand, multiple calibration at different times allows a check on whether the radiometer is drifting.

The uncertainty of the counts comes from the digitization steps and the noise. The uncertainty in the calculated radiances results from uncertainty of the optical parameters used and from imprecision of the calculation procedure.

The uncertainty from the digitization steps of the counts cannot be reduced at a single count; an improvement in this aspect of the calibration is only possible by using more counts. To keep the uncertainty in the radiances small, actual data and a good computer code must be used. Again improvement in the calibration curve or a check on the individual calibration values is possible by using more calibration values.

Such an improvement is simplest for radiometers which respond linearly to the incoming radiation. Then, as mentioned above, the result of the calibration procedure is one calibration constant, the slope of the straight line determined from the calibration values. The divergence of the calibration values from the line

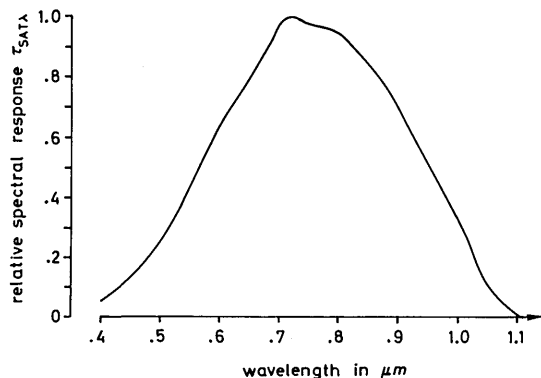


Fig. 1. Spectral response of the Meteosat-1 channels VIS-1 and VIS-2.

gives a check on their validity and so on the validity of the optical data taken from the atmosphere and the reflectances. Statistical uncertainties of the data result in a lower regression coefficient but not in uncertainty in the calibration constant. However, systematic errors would change the slope of the straight line and so give an error in the calibration constant.

If deep space measurements fix the intersection point, an additional improvement is given, because then the calibration values only determine the slope of the straight line and not its complete equation.

To get absolute radiances, values of the spectral irradiance of the sun at the top of the atmosphere are used in the calculations. Since a possible uncertainty of these solar data results in a systematic error in all radiances, it also results in the same error in the calibration constant. The uncertainty in the solar spectral irradiance also acts, of course, in all other calibration procedures which use the sun as a source. But in principle, this uncertainty is no weakness in a calibration method, because it can be assumed that solar values will certainly be redetermined with high precision in the future. Possible rapid variations¹⁰ of the solar constant or its spectral distribution are at least very small and can be neglected compared with other uncertainties.

IV. Application to Meteosat-VIS-Channel

The European geostationary satellite Meteosat-1⁸ was launched in Nov. 1977 to a position at 0° longitude. It formed part of the global network of geostationary satellites distributed around the equator. Meteosat-1 was operational until Nov. 1979. As a substitute, Meteosat-2 was launched with a similar radiometer in June 1981.

The principal payload of Meteosat-1 was a multi-spectral radiometer⁸ with a channel in the thermal IR, a channel in the water vapor absorption band, and two identical channels in the solar spectral region, the VIS-channels. In the data processing procedure the European Space Operation Centre (ESOC) adjusted both channels¹¹ to give the same signal, and so they are not distinguished in the following. The instantaneous FOV of the VIS-channel is 2.5 km. Figure 1 shows the nearly triangular shape of the spectral response $\tau_{\text{sat}\lambda}$ of the VIS-channel of Meteosat-1.

Here the method of vicarious calibration is applied to calibrate this channel. The calibration is to be understood as the determination of the relation between the effective radiances L_{sat} and the Meteosat-VIS-channel output in counts, since the effective radiances are converted into counts by the measuring device.

The effective radiance L_{sat} is the integral over the incoming spectral radiances $L_{T\lambda}$ weighted with the spectral response $\tau_{\text{sat}\lambda}$:

$$L_{\text{sat}} = \int_0^{\infty} L_{T\lambda} \cdot \tau_{\text{sat}\lambda} \cdot d\lambda. \quad (2)$$

From preflight measurements¹² it is anticipated that the Meteosat-VIS-channel responds linearly. Therefore, as mentioned above, the relation between radiances and counts is given by a straight line, which slope is the calibration constant c_{sat} .

The Meteosat-VIS-channel output is originally digitized into 6-bit counts.¹³ To make use of data similar to those of the Meteosat-IR-channel, the data processing procedure by ESOC adds 2 bits to each count.¹³ Thus the users start with 8-bit counts. For each pixel, the original 6 bits of information can be extracted from these 8-bit counts by canceling the last 2 bits. In this paper all the data are reduced to these original 6-bit counts, and the calibration is made for these data.

The digitization in the Meteosat-VIS-channel gives counts equal to 1 or more for any detector output voltage higher than -5 mV (Ref. 12); consequently count 1 stands for small radiances including radiance zero. Thus the intersection point of the calibration straight line with the count axis is at the count 0.5 (see Fig. 6), and the resulting equation is given as

$$L_{\text{sat}} = c_{\text{sat}6} \cdot [(6\text{-bit count}) - 0.5], \quad (3)$$

where $c_{\text{sat}6}$ is the calibration constant for 6-bit counts.

For the 8-bit digitization it follows that count 4 stands for zero radiance, and consequently the intersection point is at count 2. The calibration constant for 8-bit counts is $c_{\text{sat}8}$; the resulting calibration equation is

$$L_{\text{sat}} = c_{\text{sat}8}[(8\text{-bit count}) - 2]. \quad (4)$$

Because the calibration relates counts to effective radiances, it does not depend on the spectral composition of the signal. As mentioned in Sec. II it is possible to use completely different targets, different atmospheric conditions, and different angles to determine the calibration constants $c_{\text{sat}6}$ and $c_{\text{sat}8}$ and so to minimize their uncertainties.

Counts were selected from deep space and from four surfaces which are homogeneous and for which the reflection functions are available. These surfaces are rough ocean,¹⁴ the savanna in Namibia,¹⁵ pasture land in northern Germany,¹⁵ and freshly fallen snow.¹⁶ The values of the optical parameters of the atmosphere are derived from my measurements and from assumptions based on air mass trajectories, values of horizontal visibility, and radiosonde data. Values for the extraterrestrial sun are taken from Neckel and Labs¹⁷ (for more details see Sec. VII).

V. Conversion Factors

The spectral radiances $L_{T\lambda}$ used in Eq. (2) also can be used to calculate integrated radiances L_T , not weighted with any spectral response:

$$L_T = \int_{\lambda_1}^{\lambda_2} L_{T\lambda} \cdot d\lambda. \quad (5)$$

The values L_T depend on the wavelength interval λ_1 to λ_2 and on the spectral behavior of $L_{T\lambda}$, i.e., on the optical properties of the atmosphere and surface.

There is great interest in absolute radiances derived from Meteosat-VIS-channel counts, e.g., for use in radiation budget studies.^{18,19} In this case radiances in the total solar spectral range L_{sol} are needed. To get L_{sol} integration over the wavelength region from ~ 0.3 to $3.0 \mu\text{m}$ is necessary:

$$L_{sol} = \int_{0.3}^3 L_{T\lambda} \cdot d\lambda. \quad (6)$$

For atmosphere and surface types, for which the optical properties are known in this broad spectral range, the radiances L_{sol} can be calculated for all directions of sun and satellite as well as the radiances L_{sat} [see Eq. (2)]. So conversion factors f_{sol} can be computed, which allow the derivation of L_{sol} from L_{sat} simply by multiplying:

$$L_{sol} = f_{sol} \cdot L_{sat} = f_{sol} \cdot c_{sat} \cdot \text{count}. \quad (7)$$

Radiances L_{sat} which have the same value and so result in the same count may originate from different spectral radiances, depending on the optical properties of atmosphere and surface and will cause different L_{sol} values, which means that the f_{sol} factors depend on the optical properties of atmosphere and surface and on the angles of sun and satellite.

As an example, values of f_{sol} are presented in Fig. 2 against the satellite elevation angle for three values of the azimuth difference φ between sun and satellite. The values are given for a clear atmosphere ($T_{0.55} = 1.5$) over a blue ocean²⁰ and medium high sun ($h_{\odot} = 57.5^\circ$) and for a turbid atmosphere ($T_{0.55} = 5$) over a green ocean²⁰ illuminated by a low sun ($h_{\odot} = 17.5^\circ$) to demonstrate the influence of different conditions. f_{sol} values for other surface types and atmospheric conditions will be presented in a subsequent paper.

As seen in Fig. 2, the factors f_{sol} are high for a clear atmosphere over a blue ocean outside the sunglint, in this figure at $\varphi = 90$ and 180° from the nadir point. This is due to the relatively high contribution of Rayleigh scattering which leads to a fast decrease of the radiances with increasing wavelength. As a result, the signal L_{sat} represents only about a quarter of the total radiance L_{sol} , and consequently the f_{sol} values are high. At higher atmospheric turbidity, over green water or in the sunglint, the radiances at longer wavelengths become comparatively higher and so do the L_{sat} values. Therefore, the f_{sol} values are smaller. Naturally the influence of the sunglint is especially pronounced in a clear atmosphere, as Fig. 2 shows.

If radiances of a spectral interval other than the total solar region are desired, Eq. (5) can also be used. For

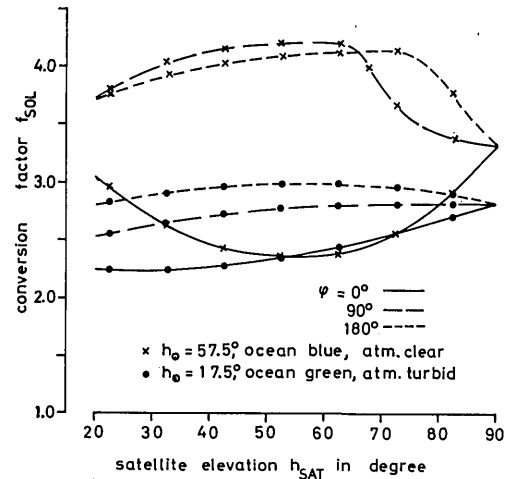


Fig. 2. Conversion factors f_{sol} [see Eq. (7)] against the satellite elevation h_{sat} for three azimuth angles φ . The two groups of curves correspond to a clear atmosphere \times ($T_{0.55} = 1.5$) with maritime aerosol²⁸ of 70% relative humidity over a blue ocean²⁰ with waves²⁴ illuminated by a medium high sun and to a rather turbid atmosphere \bullet ($T_{0.55} = 5$) with the same aerosols²⁸ over a green ocean¹⁴ illuminated by low sun. In both cases, the amount of water vapor is 3 g/cm^2 , and of ozone is $6.4 \times 10^{-4} \text{ g/cm}^2$ ($\approx 0.3 \text{ atm-cm}$).

example, Kriebel⁵ measured radiances with a rectangular filter between 0.4 and $1.1 \mu\text{m}$, which are the approximate limits of the Meteosat-VIS-channel (Fig. 1). This radiance L_{rec}

$$L_{rec} = \int_{0.4}^{1.1} L_{T\lambda} \cdot d\lambda \quad (8)$$

can again be calculated from L_{sat} , in this case with the corresponding conversion factor f_{rec} :

$$L_{rec} = f_{rec} \cdot L_{sat} = f_{rec} \cdot c_{sat} \cdot \text{count}. \quad (9)$$

For the same reasons as for the f_{sol} factors, these f_{rec} factors depend on the optical conditions of atmosphere and surface and on the angles of sun and satellite. As a consequence, the appropriate f_{rec} value must be used if L_{rec} is to be determined from Meteosat counts.

The f_{rec} values are small if L_{sat} values are high compared with the L_{rec} values and vice versa. It follows, for example, that f_{rec} has small values if the spectral radiances $L_{T\lambda}$ are high around the peak in the spectral response curve τ_{sat} .

In Figs. 3–5 for three surfaces f_{rec} values are plotted against the satellite elevation angle for three values of the azimuth and for a low and medium high sun.

Radiances over dark ocean surfaces outside the sunglint are an example of low $L_{T\lambda}$ values at wavelengths near the peak of τ_{sat} . In Fig. 3 f_{rec} values valid for such conditions are presented. As in Fig. 2, the values are given for a clear atmosphere over a blue ocean and medium high sun and for a turbid atmosphere over a green ocean with low sun. The behavior of the f_{rec} values can be explained in the same way as the behavior of the f_{sol} values in Fig. 2 and is not repeated.

An example of high $L_{T\lambda}$ values around the peak in the spectral response is provided by radiances over green

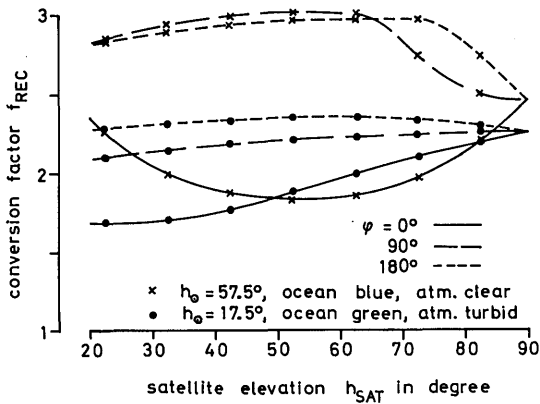


Fig. 3. Conversion factors f_{rec} [see Eq. (9)] against the satellite elevation h_{sat} . The parameters are the same as in Fig. 2.

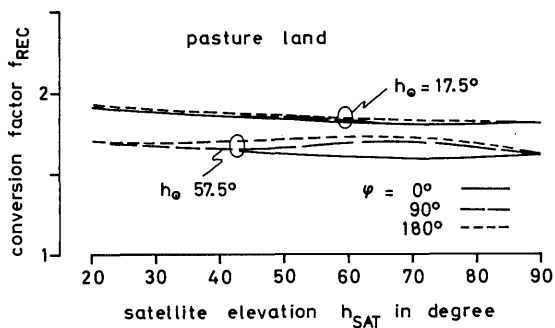


Fig. 4. Conversion factors f_{rec} [see Eq. (9)] against the satellite elevation h_{sat} . The different curves correspond to azimuth and solar elevation h_0 . The atmosphere has medium turbidity ($T_{0.55} = 2.5$) with maritime aerosol²⁸ of 70% relative humidity over pasture land.¹⁵ Water vapor is 3 g/cm^2 ; ozone is $6.4 \times 10^{-4} \text{ g/cm}^2$ (0.3 atm-cm).

pasture land. f_{rec} values for this case and mean atmospheric turbidity are shown in Fig. 4. The values are clearly lower than the values over water outside the sunglint. A small variation can be seen with variation of the solar elevation angle. At low solar elevation the scattering processes in the atmosphere become more important, the signal tends more to the blue, and so the f_{rec} values become greater.

Figure 5 shows f_{rec} values for the savanna as the underlying surface. The behavior of the values can again be explained from the color of the radiances at the top of the atmosphere.

In case of clouds, the reflection properties are nearly wavelength independent in the visible.²¹ So the spectral radiances $L_{T\lambda}$ show the same spectral behavior as the irradiance of the sun if scattering above the cloud is neglected. Under this assumption, a value $f_{rec} = 1.88$ is the result. If some Rayleigh scattering is taken into account, the radiance will be shifted to the blue, and so $f_{rec} = 1.9-2.0$ will be a good value over clouds. A more detailed investigation of the f_{rec} values will also be given in the paper announced.

VI. Numerical Treatment

Calculation of spectral radiances $L_{T\lambda}$ emerging from the top of the atmosphere is performed by a successive order of scattering program,²² which accounts for all orders of scattering and neglects polarization effects. Spectral bidirectional reflection functions for different surfaces can be used. The spectral scattering phase functions are calculated with a Mie computer program²³ which accounts for particles as homogeneous spheres. To get spectral radiances at small wavelength intervals, radiances are calculated at five wavelengths with a value of the irradiance of the sun equal to 1. Because of the slow variation of the optical properties of the scattering particles with wavelength, these radiances can be interpolated to get radiances at all wavelengths. Finally the true irradiance of the sun is considered allowing determination of $L_{T\lambda}$ at twenty-nine wavelengths.

The integration over the wavelength [Eq. (2)], which yields L_{sat} , is performed at $0.025\text{-}\mu\text{m}$ intervals. The absorption of H_2O , O_2 , and O_3 is accounted for using the method of expansion of the gas transmission functions into exponential series.^{24,25} It is found, for example, that water vapor reduces the upward emerging radiances in the Meteosat-VIS-channel by up to 15% when green pasture land is the underlying surface.

The calculation procedure is checked by comparing calculated and measured radiances.²⁶ The agreement of the radiances in the Meteosat-VIS-channel from the top of the atmosphere is good.

To save computer time, the radiances are calculated for six solar elevations, twenty-five satellite elevations, and forty azimuths. For the actual angles, radiances are interpolated from these values.

VII. Determination of Atmospheric and Surface Parameters

Actual values of the relevant optically acting parameters of the atmosphere and the earth's surface are needed for the vicarious calibrations by means of calculated radiances.

Such values were measured on cloudfree days between Apr. and Sept. 1979 at the research platform North Sea (54.7°N and 7.2°E). This position is very

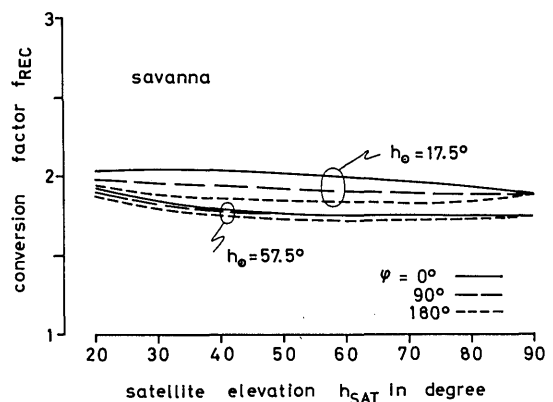


Fig. 5. Conversion factors f_{rec} [see Eq. (9)] against the satellite elevation h_{sat} . Parameters are the same as in Fig. 4, except for continental aerosol²⁸ over savanna,¹⁵ water vapor: 1 g/cm^2 .

suitable, because the corresponding pixel in the Meteosat picture is well out of the sunglint, and because the amount of air light is high and varies with the sun's height, which gives independent calibration values. Spectral values of the aerosol optical thickness were measured on the platform²⁷ at ten wavelengths between 0.43 and 2.16 μm . The aerosol types were derived from air mass trajectories; the corresponding size distributions and refractive indices were taken from Hänel and Bullrich.²⁸ The resulting spectral extinction measurements agree well with the *in situ* results. The reflection functions of the ocean surface were calculated after Cox and Munk¹⁴ from the actual wind velocities. The radiation backscattered into the atmosphere from inside the water was measured at five wavelengths between 0.443 and 0.75 μm . It was taken into account as well as the usual low coverage of the surface with whitecaps determined by a photographic method.²⁹

To get additional independent calibration values, an area with pasture land in northern Germany ($\sim 53.5^\circ\text{N}$, 7.5°E) and the savanna in Namibia ($\sim 18^\circ\text{S}$, 17°E) were used as horizontally homogeneous surfaces, for which reflection functions are known.¹⁵

The calibration values from pasture land were taken from the end of May until July 1979. The spectral bidirectional reflection functions¹⁵ were supplemented with information on its spectral behavior.³⁰ Since the summer was wet in northern Germany, the meadows kept green during the period and could be assumed to be represented well by the reflection functions. The aerosol properties taken into account were the same as those measured at the North Sea platform after considering the air mass trajectories.

Calibration values from the savanna were taken in Sept. 1979. This was the same part of the dry season that Kriebel¹⁵ used for his measurements.

For the savanna, the optical thickness was derived from actual visibility values³¹ together with the aerosol height distribution.³² The aerosol type was continental according to the air mass trajectories. Extinction coefficients calculated from the corresponding aerosol data²⁸ agree with measurements³³ carried out in 1971.

A surface covered with freshly fallen snow in northern Germany ($\sim 54^\circ\text{N}$, 10°E) was used as an underlying surface 6 Feb. 1979. Its reflectance was assumed to be an isotropic reflector with a spectral albedo after Kondraty.¹⁶ This can be taken as correct, because the snow was deep (more than 50 cm), having fallen the night before, and the backscattered radiance was analyzed. The corresponding optical properties of the atmosphere were derived from air mass trajectories and visibility measurements.

In each case the influence of the air molecules was accounted for by the barometric pressure at ground level. Ozone^{34,35} and oxygen³⁶ were taken to have their climatological values. The amount of water vapor in the vertical column was calculated from data of the nearest radiosonde. Its band transmission was derived using the equation from Moskalenko³⁷ and the data from Koepke and Quenzel.³⁸

Values of the irradiance of the extraterrestrial sun were taken from Neckel and Labs¹⁷ and corrected with factors to account for variation of the distance between sun and earth in the course of the year.³⁹

The elevation of Meteosat at the targets varied from 27° over the North Sea to 60° over the savanna. Solar elevations varied between 15° in the morning and in the evening and more than 65° at noon. The azimuth difference between sun and satellite azimuth ranged from $\sim 70^\circ$ in the morning to 180° near noon.

To get additional information about the calibration straight line, counts from deep space were used.

VIII. Resulting Calibration Constant

In Fig. 6 the effective radiances L_{sat} , calculated from the actual data of the relevant optical properties of the atmosphere and the surface, are plotted against the corresponding 6-bit counts of the Meteosat-VIS-channel; i.e., the independent calibration values are plotted.

Only values from cloudfree pixels are shown. Nevertheless, a few calibration values from clouds were derived. For example, a very bright tropical cloud showed a 6-bit count of 46 at a solar elevation of 76° . A corresponding effective radiance of $122.5 \text{ W} \cdot \text{m}^{-2} \cdot \text{sr}^{-1}$ was calculated based on an albedo of 80%. In fact these calibration values fit well onto the straight line, which is composed of the calibration values of the other surfaces. Despite the good fit, the clouds are not used to derive the calibration constant because of uncertainties

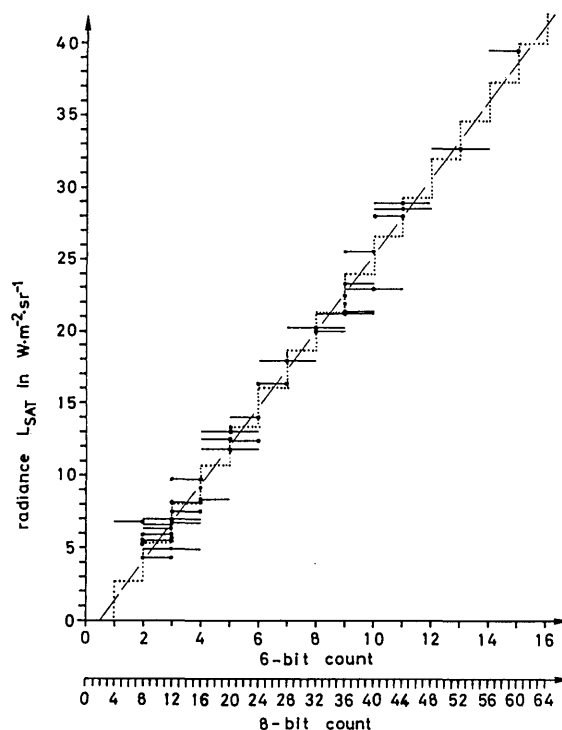


Fig. 6. Effective radiance L_{sat} [see Eq. (2)] over corresponding counts of the Meteosat-VIS-channel \bullet . The counts are presented as 6- and 8-bit data. The dotted step curve represents the digitization steps of the 6-bit counts. The slope of the broken straight line represents the calibration constant $c_{\text{sat}} = 2.66 \text{ W} \cdot \text{m}^{-2} \cdot \text{sr}^{-1}/(6\text{-bit count})$.

due to their local optical properties. Therefore, only counts with values lower than 16 are used, and the 6-bit count axis ends at this value. The 8-bit scale is presented as an additional axis, and it is curtailed for the same reason.

The counts are taken over the ocean surface from histograms of 400 pixels ($\sim 125 \times 55$ km in the German Bight), of 90 pixels over the pasture land and the snow ($\sim 30 \times 50$ km in northern Germany), and of 3200 pixels over the savanna ($\sim 105 \times 210$ km in northern Namibia). The size of these areas is adapted to the homogeneity of the surfaces. As a result the histograms usually have less than three columns. For the calibration the counts with highest frequency are used. If the frequency of the counts in the histograms is higher than 60%, they are marked in Fig. 6 by a dot. If there are two counts with nearly the same frequency between 40 and 50%, two dots are plotted and connected with a line. A horizontal line is plotted without dots, to mark counts with a frequency of <40% but more than 20%. Other counts with lower frequency occur in a few cases but are not representative and not shown in Fig. 6. The counts from deep space are also not shown. As mentioned in Sec. III, they are only used to check the intersection point of the straight line with the abscissa.

In order not to overload the figure, error bars for the radiances are not given, but the inaccuracy of these values and of the resulting calibration constant is discussed in Sec. IX.

Obviously the calibration values can be fitted well to a straight line, which is in agreement with the linear response of the Meteosat-VIS-channel as reported above. The linear regression results in a slope of 2.64; the intersection point at the abscissa is at 0.47 counts.

If the intersection point is fixed at 0.5 counts, which is right from the deep space data, the regression results in a slope of 2.66, which becomes the calibration constant for 6-bit counts:

$$c_{\text{sat}6} = 2.66 W \cdot \text{m}^{-2} \cdot \text{sr}^{-1} / (\text{6-bit count}). \quad (10)$$

Consequently the calibration constant for 8-bit counts is

$$c_{\text{sat}8} = 0.665 W \cdot \text{m}^{-2} \cdot \text{sr}^{-1} / (\text{8-bit count}). \quad (11)$$

To calculate radiances from 6-bit counts, Eq. (3) has to be used and from 8-bit counts [Eq. (4)].

The calibration was made during the summer of 1979, i.e., the last quarter of the lifetime of Meteosat-1. All counts are measured by the Meteosat-1 radiometer with a gain called gain 0. The resulting calibration constants $c_{\text{sat}6}$ and $c_{\text{sat}8}$ are valid for this period and gain.

IX. Accuracy of the Calibration of the Meteosat-VIS-Channel

The accuracy of the calibration is considered for the 6-bit counts, i.e., $c_{\text{sat}6}$. Since the 8-bit counts are directly derived from these data (Sec. IV) the accuracy for $c_{\text{sat}8}$ is the same.

The calibration constant is calculated as the slope of a straight line, which is composed of forty-three inde-

pendent calibration values and additional values from deep space. The regression coefficient is 0.998.

Unfortunately the calibration is not as good as expected from the high-regression coefficient. The broad digitization steps of the Meteosat-VIS-channel result in an uncertainty that cannot be ignored.

The dotted steplike curve in Fig. 6 shows the 6-bit digitization steps. More than 91% of the calibration values lie on this curve, which shows that the calibration is good. (Calibration values from counts with nearly the same frequency in the histogram, marked by two dots connected with a line, are said to meet the curve if one dot meets the curve.)

To test the uncertainty resulting from the digitization, the calibration constant was varied by $\pm 5\%$. The increased constant results in a steeper step curve, which is matched by 79% of the calibration values. The flatter step curve, based on the decreased calibration constant, is matched by 74% of the calibration values. This reduction is evident, but, because the number of calibration values is not high enough to be unequivocal, the uncertainty of $\pm 5\%$ is assumed to be valid in the calibration constant.

Beside this inaccuracy in c_{sat} due to the counts, the radiances also give rise to an uncertainty. Possible differences between the calculated radiances and those really measured by the radiometer and converted into the corresponding counts are called errors of the radiances. If these errors are random at different calibration values, they do not change the slope of the straight line, and so no inaccuracy in c_{sat} results. However, if these errors are systematic, the slope will vary, which makes c_{sat} inaccurate. Errors in L_{sat} depend on the uncertainties (1) in the values of the solar irradiance, (2) in the spectral response of the channel, (3) in the calculation procedure, and (4) in the optical data of atmosphere and surface.

(1) Values of the spectral solar irradiance from Neckel and Labs¹⁷ are used, which have an error not higher than 1%. Moreover only the error averaged over the broad Meteosat-VIS-channel (Fig. 1) becomes effective in the calibration constant. The factor accounting for the variation of the distance between sun and earth during the year can be assumed to be precise. Thus the uncertainty in the c_{sat} values due to the irradiance of the sun can be said to be 1% or less.

(2) An uncertainty in the spectral response $\tau_{\text{sat}\lambda}$ of the radiometer gives an uncertainty in the effective radiances L_{sat} . Errors in τ_{sat} are not published. Thus the resulting error in c_{sat} can only be estimated. As a drastic assumption, the τ_{sat} values for wavelengths lower than $0.725 \mu\text{m}$ (the maximum of τ_{sat}) are decreased by 10%, and the τ_{sat} values for longer values are increased by 10% and vice versa. The resulting L_{sat} values decrease or increase, depending on the spectral composition of the signal, i.e., for different surface types. The resulting slope of the straight line would become 2.5, and 2.71 respectively, but only 84%, (85%) of the calibration values would lie on the resulting step curve. This means that the assumption of the uncertainty in the τ_{sat} values will be too strong. Nevertheless an uncertainty

in c_{sat} of 2% will be assumed, which corresponds to the variation of the slope mentioned above.

From the uncertainty in the τ_{sat} values no uncertainty results in the radiances L_{sol} and L_{rec} (Sec. V), the quantities users want to work with. These radiances can be calculated with the help of the conversion factors f_{sol} and f_{rec} together with c_{sat} from the Meteosat-VIS-counts. These conversion factors are calculated with the same spectral response as used in calculation of the L_{sat} values. Thus if c_{sat} together with f_{sol} or f_{rec} is used, no uncertainty due to the spectral response remains in the resulting radiances. The same, of course, is valid if f_{sol} or f_{rec} values are taken from any other author as long as he uses the same τ_{sat} values.

(3) The calculation accuracy of the multiple-scattering program²² is better than 1%.⁴⁰ Neglecting the polarization may account for an additional inaccuracy in the spectral radiances of <3% as concluded after Tanaka⁴¹ and Eschelbach.⁴² The determination of the band transmission of the atmospheric gases and their expansion into an exponential series lead to 5% uncertainty in the calculated gas absorption. But this absorption reduces L_{sat} under normal conditions by no more than 15%. Therefore, the resulting uncertainty in L_{sat} is <0.8%. The interpolation over the wavelengths is executed with an accuracy of better than 2%. For the interpolation over the angles, the resulting uncertainty is <1%.

All these errors lead to statistical errors in the calibration values because very different parameter conditions and angles are used. To be on the safe side, a remaining systematic error of 1% in L_{sat} is assumed, which results in the same error in c_{sat} .

(4) Errors in L_{sat} follow from the inaccuracy of the turbidity values due to measuring errors or due to uncertainties in the aerosol height distribution. In some cases, the aerosol type could not be determined with certainty. Errors can also result from this type, that is, from the phase function and the single scattering albedo used. The error in L_{sat} due to these sources of error is up to $0.7 \text{ W} \cdot \text{m}^{-2} \cdot \text{sr}^{-1}$.

Errors in L_{sat} from the inaccuracy of the amount of water vapor are <2%, because data from the nearest radiosonde are used. Ozone reduces the signal no more than 2%, so its difference from the climatological values can be ignored.

The uncertainty in L_{sat} caused by the reflection function of the water surface can be assumed to be 2% or less because the values are taken outside the sunglint, where its contribution to the signal at the satellite is low. Furthermore, measured values are used for the amount of whitecaps and for the underlight. The inaccuracy of the reflection functions of the land surfaces is high in the short-wavelength region.¹⁵ But taking into account the spectral response of the radiometer and the path radiance, the resulting uncertainty in L_{sat} is 2%. It must be stressed that bidirectional reflection functions are used in the calculations, which is necessary because the assumption of a Lambertian reflector for the land surfaces would lead to an unacceptable error in the radiances of up to 25%.⁴³ The uncertainty in L_{sat}

caused by the reflection function of the snow covered surface is assumed to be no more than 3%, because the snow is fresh, the conditions of the published values are fulfilled, and the sun is rather low; i.e., the contribution of the path radiance is high.

All these errors are statistical and so do not result in an error in c_{sat} . Only the error of the reflection function of the land surfaces may be systematic, because these data all were measured with the same radiometer. However, the calibration of this radiometer should not show an error in the same direction in all channels. Nevertheless to account for possible small additional differences between the actual and the used reflection functions, a 3% uncertainty in c_{sat} owing to knowledge of the optical data is assumed.

The different possible systematic errors in the calibration values are independent and so can be combined as root sum square to the total inaccuracy of c_{sat} , which is $\pm 6.3\%$. As mentioned above, the error in c_{sat} based on the inaccuracy of the spectral response of the Meteosat-VIS-channel will not cause an error in L_{rec} and L_{sol} . So the total error in the product c_{sat} multiplied by f_{rec} or f_{sol} , i.e. the total error of the vicarious calibration presented in this paper is $\pm 6\%$.

In addition to the error caused by the inaccuracy of the calibration discussed above, radiances determined from the counts have an error of plus or minus half a count owing to the digitization steps of the radiometer. The resulting error in the radiances is $\pm 1.3 \text{ W} \cdot \text{m}^{-2} \cdot \text{sr}^{-1}$, which is rather high at low radiances.

X. Comparison with Other Calibrations

Results of the calibration presented here can be compared with results of (1) Möser *et al.*,¹⁹ which is a constant equivalent to c_{sat} , and (2) Kriebel,⁵ which are calibration factors equivalent to f_{rec} multiplied by c_{sat} , and so depend on the state of the atmosphere and the surface.

(1) The calibration constant presented by Möser *et al.*¹⁹ is evaluated for their use of Meteosat counts to determine the radiation balance in the solar spectral region. Their calibration was similar to this paper but with only six data pairs, all taken over the Sahara. The reflection function is taken as an isotropic albedo; other data for the calculations are not reported. To compare radiances and counts they use a straight line crossing the origin of the coordinates. Their resulting calibration constant equivalent to c_{sat} is $2.42 \pm 0.16 \text{ Wm}^{-2} \text{sr}^{-1}/(6\text{-bit count})$. If they were to use the better value of 0.5 counts as an intersection point, their resulting constant becomes 2.48.

(2) Kriebel⁵ calibrates the Meteosat-VIS-channel by comparing counts with corresponding radiances L_{rec} , measured with a calibrated instrument from a high-altitude aircraft. With a radiometer which always looks in the same direction as Meteosat, radiances over four surface types (Table II) are taken, averaged over the flight pattern. In each case, a calibration factor is calculated as the slope of the straight line, determined by the single data pair of count and radiance and by the origin of the coordinates.

Table II. Calibration Factors of the Meteosat-VIS-Channel (6-bit Counts) Compared with Results from Kriebel⁵

Target type	Conversion factors (f_{rec})	This study	Kriebel ⁵
		Calibration factors ($f_{\text{rec}} \cdot c_{\text{sat}}$) [see Eq. (9)] (%)	calibration factors (u_c) (%)
Land surface	1.6–1.8	4.26–4.79 ± 6	5.16 ± 5
Stratocumulus	1.9–2.0	5.05–5.32 ± 6	5.40 ± 5
Atlantic Ocean	2.9–3.0	7.71–7.98 ± 6	9.60 ± 20
Mediterranean Sea	2.5–2.8	6.65–7.45 ± 6	8.00 ± 20

As mentioned above, a specific count may lead to different L_{rec} values under different conditions due to the spectral response of the radiometer. Thus Kriebel's calibration factors, called u_c here, vary like the f_{rec} values with the spectral composition of the radiances L_{rec} , which he used for his calibration.

This means that Kriebel's calibration factors u_c can only be applied directly to those types of surface where comparison measurements have actually been made.⁵ The same restriction holds for the other conditions which determine the color of the radiances at the actual comparison measurements. Thus the calibration factors u_c are valid only for specific angles of sun and satellite and for specific conditions of atmosphere and surface. From Eq. (9) the following equivalence is deduced:

$$u_c = f_{\text{rec}} \cdot c_{\text{sat}} \quad (12)$$

In Table II together with Kriebel's u_c values corresponding products of c_{sat} times f_{rec} are presented, which allow a comparison of the result of this paper with Kriebel's results. To obtain the right f_{rec} values, the angles of sun and satellite are taken from the position and time of flights. The uncertainties in the f_{rec} values from the uncertainties of the reflection function and atmospheric state are considered in Table II as a variability range for the f_{rec} values. For the atmospheric aerosol, mean conditions are used, because no actual data are available. For the land surface, La Mancha in Spain, which is treeless with wheat, corn, and sunflowers, f_{rec} values calculated from the savanna (which may agree in color) as well as from the pasture land (which may agree in structure) are taken into account. Of course, in this case the right f_{rec} value may still be different. However, the f_{rec} values for the cloud and for the sea surfaces will be correct.

The comparison in Table II shows that Kriebel's u_c values in all four cases are higher than the corresponding result from this paper, especially for the water surfaces. This behavior can be explained as due to the accuracy of the data.

The accuracy of my result is 6.3%, as discussed in Sec. IX. The measuring accuracy of Kriebel is 5%. However, he gets an additional inaccuracy due to the broad digitization steps of Meteosat, which is ~20% over water as an underlying surface,⁵ owing to low radiances in this case. Since each calibration factor by Kriebel is derived from only one pair of radiance and count, the uncer-

tainty from the digitization yields the same uncertainty in his calibration factors. Considering this inaccuracy, the agreement in Table II is good.

XI. Summary and Conclusion

The method of vicarious calibration by means of calculated radiances allows for any spectral region the calibration of satellite-borne radiometers including the complete optics. This paper shows that the method can be used successfully in the solar spectral range.

In the case of radiometers with gray flat spectral response or with small interference filters and with linear response, the result is one calibration constant. This constant is evaluated by comparing counts of the radiometer with corresponding radiances, which are calculated on the basis of actual values of the optically acting parameters of the atmosphere and the earth's surface and on deep space measurements. Repeated calibration during the lifetime of the radiometer would allow the drift in its response to be followed.

In the case of radiometers with broad response but not gray, the effective radiance (the radiance weighted with the spectral response) which is converted into counts depends on the spectral composition of the signal. An example of such a nonrectangular response curve is the VIS channel of Meteosat, the calibration of which is presented in this paper. A specific count from such a nongray radiometer (i.e., a specific effective radiance) may result from different radiances at the satellite (radiances not weighted with the spectral response) due to a different spectral composition.

Therefore, for radiometers with a broad nongray response, the calibration is separated into two steps: (1) Determination of the calibration constant, which describes the absolute calibration. This constant can be derived in the same way as the constant for a radiometer with gray response and also can be used to monitor a possible drift of the radiometer.

(2) The second step is determination of conversion factors, which connect the effective radiances with radiances at the satellite not weighted with the spectral response of the radiometer. These conversion factors depend on the spectral composition of the signal, i.e., on the optical properties of the atmosphere and the earth's surface and on the geometry. They can be calculated for all possible sets of these parameters.

For the Meteosat-VIS-channel, conversion factors f_{sol} [Eq. (7)] and f_{rec} [Eq. (9)] are presented with a few examples. They allow either determination of the radiance at the satellite in the total solar range L_{sol} or of the radiance at the satellite in the spectral range between 0.4 and 1.1 μm L_{rec} . To use the correct conversion factors, knowledge of the actual values of the optical parameters of the atmosphere and the surface is necessary. This knowledge is poor in many cases. A subsequent paper will give conversion factors for further conditions and more important a parametrization which allows the correct conversion factor to be found from the Meteosat signal itself together with day, time, and pixel position.

The calibration constant of the VIS-channel of Meteosat-1 has the value $c_{\text{sat}} = 2.66 \text{ W} \cdot \text{m}^{-2} \cdot \text{sr}^{-1}/(6\text{-bit count})$. This constant is valid, at least for summer 1979, the last quarter of the lifetime of the radiometer. It is determined for the gain of the radiometer, called gain 0. The inaccuracy of the calibration is $\pm 6\%$. It is mainly due to the broad digitization steps. Since this digitization gives additional uncertainty of half a count, i.e., of $\pm 1.3 \text{ W} \cdot \text{m}^{-2} \cdot \text{sr}^{-1}$ in the radiances derived from the counts, a better digitization of the Meteosat-VIS-channel is desired.

I would like to thank K. T. Kriebel and H. Quenzel for illuminating discussions and the unknown reader for his helpful comments. I would also like to thank J. Christoffer, K. H. Werner, and the crew of the North Sea research platform for their help with the measurements. I gratefully acknowledge the technical assistance of G. Pucher and B. Beyer from the Meteorological Institute, Hamburg, T. Koenig and W. Rattei from the DFVLR, Oberpfaffenhofen, and D. Matthies-Tschernichin, E. Quenzel, and K. Nodop from the Meteorological Institute, Munich. The research was sponsored under grant MF 0235 by the German Minister of Technology and Research (BMFT).

All measurements were made at the Meteorological Institute, University of Hamburg.

References

- References 7, 8, 11, 12, 13, and 19 are prepared and distributed for the European Space Operations Centre (ESOC) by Meteosat Data Management Department (MDMD), Robert Bosch Str. 5, D61 Darmstadt, Federal Republic of Germany, Telex 419453.
- H. W. Yates, in *Programs and Abstracts IRC, Symposium on the Calibration of Satellite Instruments, 17-28 Aug. 1981* (IAMAP, Hamburg, 1981).
 - E. A. Smith and D. Loranger, "Radiometric Calibration of Polar and Geosynchronous Satellite Shortwave Detectors for Albedo Measurements," Tech. Rep., Department of Atmospheric Science, Colorado State U., Fort Collins (1977).
 - N. Beriot, N. A. Scott, A. Chedin, and P. Sitbon, *J. Appl. Meteorol.* **21**, 84 (1982).
 - M. J. Duggin, *Appl. Opt.* **20**, 3815 (1981).
 - K. T. Kriebel, *Appl. Opt.* **20**, 11 (1981).
 - For example, in the IR spectral region: P. Koepke, *Contrib. Atmos. Phys.* **53**, 442 (1980).
 - For example, in the spectral region of the 6.3- μm water vapor absorption band: J. R. Eyre, in *Proceedings, Second Meteosat Scientific User Meeting, London, 26-27 Mar. 1980* (ESOC, Darmstadt, 1980), p. A-1.
 - Meteosat System Guide, Vol. 6, Issue 1* (MDMD, ESOC, Darmstadt, 1980).
 - S. Chandrasekhar, *Radiative Transfer* (Clarendon, Oxford, 1950).
 - R. C. Willson, in *Programs and Abstracts IRC, Symposium on the Solar Constant, 17-28 Aug. 1981* (IAMAP, Hamburg, 1981), p. 145.
 - M. Jones and J. Morgan, *Adjustment of Meteosat-1 Radiometer Response by Ground Processing* (MDMD, ESOC, Darmstadt, 1979).
 - G. Lebegue, Meteosat, Dossier des etalonnages relatifs a F1, Doc. 2362-/85 TKA, Comp. Societe National Industrielle Aerospatiale, Cannes (1977).
 - J. Morgan, *Introduction to the Meteosat System* (MDMD, ESOC, Darmstadt, 1978).
 - C. Cox and W. Munk, *J. Mar. Res.* **13**, 198 (1954).
 - K. T. Kriebel, *Appl. Opt.* **17**, 253 (1978).
 - K. Y. Kondratyev, *Radiation in the Atmosphere* (Academic, New York, 1969).
 - H. Neckel and D. Labs, *Sol. Phys.* **74**, 231 (1981).
 - R. W. Saunders and G. E. Hunt, *Nature* **283**, 645 (1980).
 - W. Moser, H. J. Preuß, E. Raschke, and E. Ruprecht, in *Proceedings, Second Meteosat Scientific User Meeting, London, 26-27 Mar. 1980* (ESOC, Darmstadt, 1980), pp. K-1.
 - A. Morel, *Boundary Layer Meteorol.* **18**, 177 (1980).
 - E. M. Feigelson, *Light and Heat Radiation in Stratus Clouds*, translated from Russian (Israel Program for Scientific Translation, Jerusalem, 1966).
 - H. Quenzel, in *Daylight Illumination-Color-Contrast Tables for Full-Form Objects*, M. R. Nagel, H. Quenzel, K. Kweta, and R. Wendling, Eds. (Academic, New York, 1978).
 - H. Quenzel and H. Müller, *Optical Properties of Single Mie Particles* (Wiss. Mitt. Meteorol. Inst., U. München, 1978), No. 34.
 - M. Kerschgens, E. Raschke, and U. Reuter, *Contrib. Atmos. Phys.* **49**, 81 (1976).
 - S. Bakan, P. Koepke, and H. Quenzel, *Contrib. Atmos. Phys.* **51**, 28 (1978).
 - V. Amann, P. Koepke, and K. T. Kriebel, "Validation of Radiative Transfer Models by Comparison with Airborne Radiance Measurements," in *Extended Abstracts, Radiation Session R-1, 17-18 Aug. 1981* (IAMAP, Hamburg, 1981).
 - P. Koepke, *Eurasep Newslett.* No. 4, 13 (1981); available from Joint Research Centre, 21020 Ispra, Italy.
 - G. Hanel and K. Bullrich, *Contrib. Atmos. Phys.* **51**, 129 (1978).
 - E. L. Monahan, *J. Phys. Oceanogr.* **1**, 139 (1971).
 - K. Y. Kondratyev, Ed., *Radiation Characteristics of the Atmosphere and the Earth's Surface* (Amerind, New Delhi, 1973).
 - Weather Bureau, Windhoek, Namibia, and Weather Station, Grootfontein, Namibia; private communication (1980).
 - K. T. Kriebel, *Contrib. Atmos. Phys.* **51**, 330 (1978).
 - H. Quenzel, in *Proceedings, International Radiation Symposium, Sendai, Japan, 26 May-2 June 1972*, p. 304.
 - J. R. London, D. Bojkov, S. Oltmans, and J. I. Kelly, *Atlas of the Global Distribution of Total Ozone*, NCAR/TN 113 + STR, Boulder (1976).
 - H. U. Dütsch, in *Meteorologisches Taschenbuch*, F. Baur, Ed. (Geest & Portig, Leipzig, 1970), p. 555.
 - D. Q. Wark and D. H. Mercer, *Appl. Opt.* **4**, 839 (1965).
 - N. L. Moskalenko, *Izv. Atmos. Ocean Phys.* **5**, 678 (1969).
 - P. Koepke and H. Quenzel, *Appl. Opt.* **17**, 2114 (1978).
 - F. Baur, Ed., *Meteorologisches Taschenbuch* (Geest & Portig, Leipzig, 1970), p. 520.
 - J. Lenoble, Ed., *Standard Procedures to Compute Atmospheric Radiative Transfer in a Scattering Atmosphere, Rep. 6, Radiation Comm.* (IAMAP, Boulder, Colo., 1977), p. 125.
 - M. Tanaka, *J. Meteorol. Soc. Jpn.* **49**, 321 (1971).
 - G. Eschelbach, "Berechnungen des Strahlungsfeldes einer dunsthaltigen Atmosphäre im solaren Spektralbereich," Doctoral Thesis, U. Mainz, Mainz, Germany (1972), p. 98.
 - P. Koepke and K. T. Kriebel, *Appl. Opt.* **17**, 260 (1978).